Holography and speckle techniques for real-time displacement deformation and vibration analysis

H. J. Tiziani, J. Klenk, K. Leonhardt
Institute of Applied Optics, University Stuttgart
D-7000 Stuttgart 80, Germany

Abstract

Holographic interferometry and speckle application are powerful techniques for deformation, displacement and vibration analysis especially when they can be applied in real time. Bismuth Silicon Oxide crystals Bi_{12} Si O_{20} (BSO) were used for real-time deformation, displacement and vibration analysis using holography and "speckle photography". After a short introduction of holographic interferometry for deformation measurement using BSO crystals, speckle applications for deformation, displacement and vibration analysis in real time will be discussed.

1. Introduction

Some crystals have electrical and electro-optical properties which make them attractive for dynamic holography and speckle applications. One of the most promising is the Bismuth Silicon Oxide Bi_{12} Si O_{20} (BSO). Crystal properties and some applications were reported in the session D1 at the meeting by Huignard[1-2].

For real time holography and holographic interferometry the BSO crystal is usually biased with a transverse electric field E_o in the 110 crystallographic direction. Illuminating the crystal with structured information in the $\bar{1}10$ direction a space-charge field is built up, leading to a refractive index variation of the crystal via linear electro-optic effect. A phase volume hologram is created.

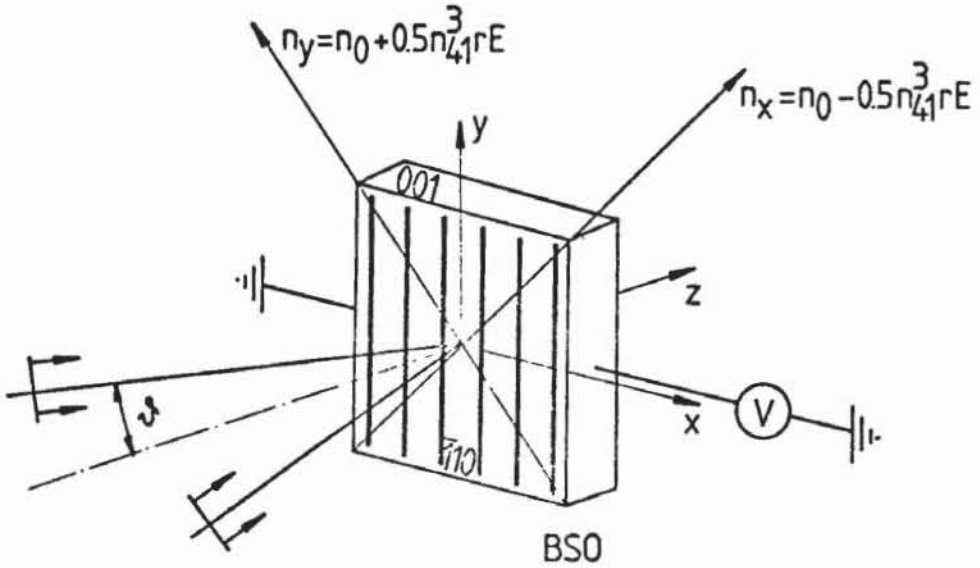

Fig. 1 BSO crystal used in a transverse electro-optic configuration

Fig. 1 shows schematically the crystal illuminated with two waves to create an interference pattern or a phase hologram in the crystal. Flooding with uniform illumination at a wavelength where the crystal is sensitive leads to the erasure of the stored information by space-charge relaxation. Consequently, reading out with the recording wavelength is destructive.

In fig. 2 a diffraction efficiency curve is drawn schematically for the writing and reading cycle. In fig. 3 the quality of a holographically reconstructed test bar target is shown. The image quality is limited by the resolution of the TV monitor.

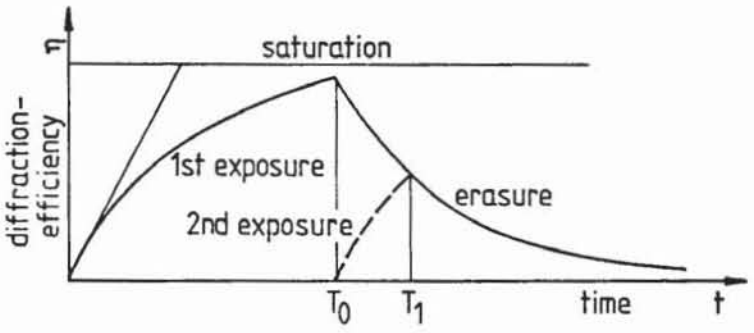

Fig. 2 Diffraction efficiency by recording and erasure in a BSO crystal

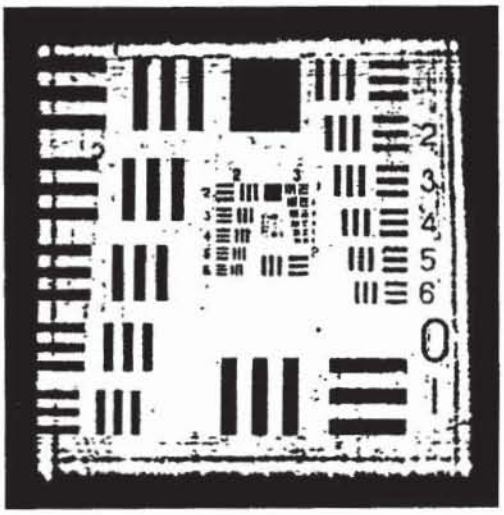

Fig. 3 Example of a real time holographic reconstruction with a BSO crystal.

2. Double exposure holography with BSO crystals

A short description of double exposure holography will be given together with a sketch of the experimental arrangement. Reading out with the recording wavelength leads to an erasure of the information stored in the crystal. Therefore, for double exposure holography the first exposure is T_o (fig. 2), the second after the object deformation is $T_1 \quad T_o/2$. This leads to two phase holograms stored in the crystal. Reconstructing the two holograms with the recording wavelength leads to an interference pattern for the deformation and displacement analysis which can be stored on an image storage device.

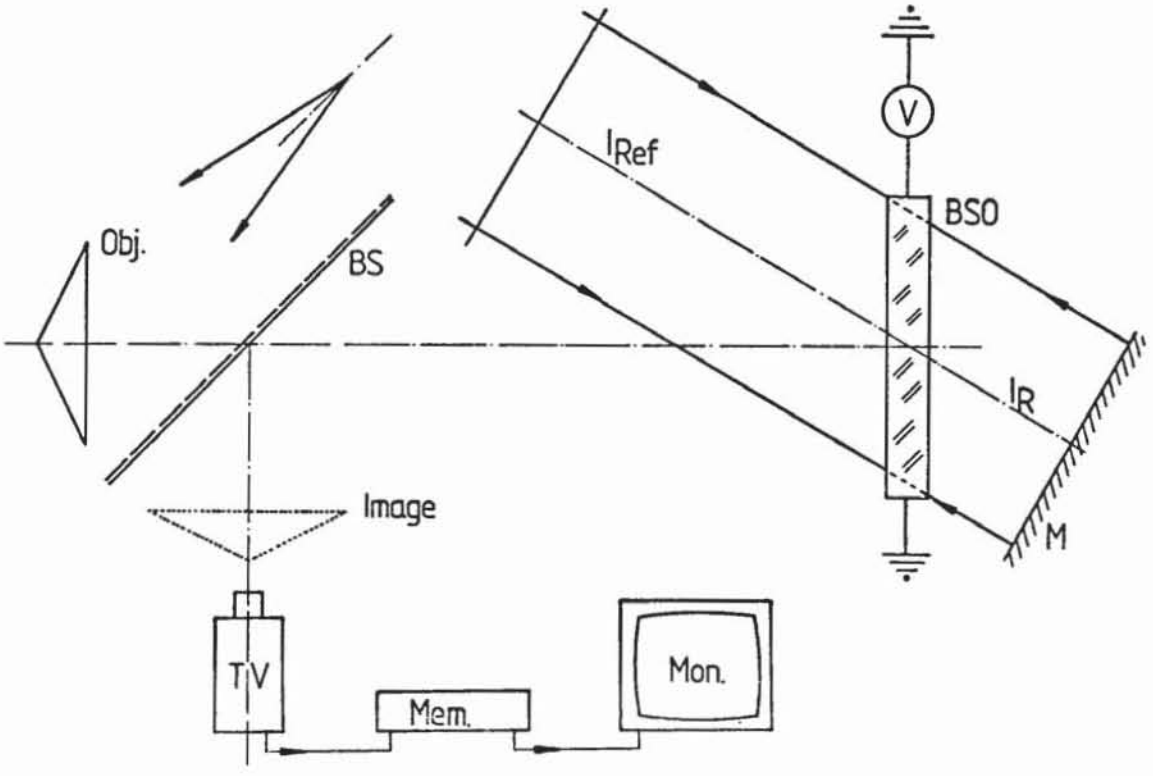

Fig. 4 Experimental arrangement for double exposure holographic interferometry in real time

Fig. 4 shows an experimental arrangement for holographic interferometry. The double exposed hologram is formed in the crystal. The reconstructing wave is the conjugate to the reference wavefront. The reconstructed image is separated from the object by the beam-splitter. Fig. 5 shows a typical fringe pattern of a deformed plate when using double exposure technique. The plate was deformed after the first exposure by the application of a force.

Fig. 5.
Example of interference fringes obtained in real time by double exposure holography of a deformed plate.

3. Speckle pattern recording in BSO crystals

For engineering applications, different speckle techniques can be applied. The choice depends mostly on the sensitivity required. The application of speckle photography in quasi real time will be discussed. The speckles in the image plane of an optically rough surface of an object are displaced together with the image at least for small movements. The roughness of the object is not resolved by the optical system. For deformation and displacement measurements pairs of speckle patterns are recorded in the crystal with wavelength λ_1. The separation of the speckle pairs should be greater than the speckle width. The two speckle patterns recorded in the crystal, before and after the object movement, are illuminated with light of a wavelength λ_2 with a crystal absorption for λ_2 to be much smaller than for the recording wavelength λ_1. The absorption coefficients of the crystals used were $\alpha = 2\ cm^{-1}$ for $\lambda_1 = 514$ nm and $\alpha_2 = 0{,}28\ cm^{-1}$ for $\lambda_2 = 633$ nm. For speckle pairs recorded in the image plane, Young's fringes with a spacing inversely proportional to the displacement are formed in the Fraunhofer plane. They can be analysed directly using television techniques. In a simplified theory the appearance of Young's fringes will be described briefly for displacement analysis by double exposure speckle pattern recording and display in real time.

The double exposed speckle pattern in the image of the lens L_1 in fig. 6 may be written by

$$I(\vec{\xi},\Delta\vec{\xi}') = B(\vec{\xi}') \circledast \{\delta(\vec{\xi}') + \delta(\vec{\xi}' - \Delta\vec{\xi}')\} \qquad (1)$$

where $B(\vec{\xi}')$ describes the speckle pattern and $\circledast$ means convolution. $\Delta\vec{\xi}' = M \cdot \Delta\vec{\xi}$ is the displacement in the image and $\Delta\vec{\xi}$ in the object with M as lateral magnification.
The refractive index Δn_s at saturation is given by

$$\Delta n_s = \left(\frac{n^3\ r\ E_{sc}}{2}\right) \qquad (2)$$

n = refractive index of the BSO (n = 2,5 for $\lambda_2 = 633$ nm)
r = effective electro-optic coefficient
E_{sc} = space-charge field amplitude derived from Poisson's equation[1]

The refractive index modulation due to the spatially structured illumination can be written

$$\Delta n = \Delta n_s \cdot \frac{I(\vec{\xi}',\Delta\vec{\xi}')}{\langle I(\vec{\xi}')\rangle} \qquad (3)$$

for a crystal of a small thickness ($d \approx 1$ mm), $\Delta n \cdot d \approx \lambda_1/40$.

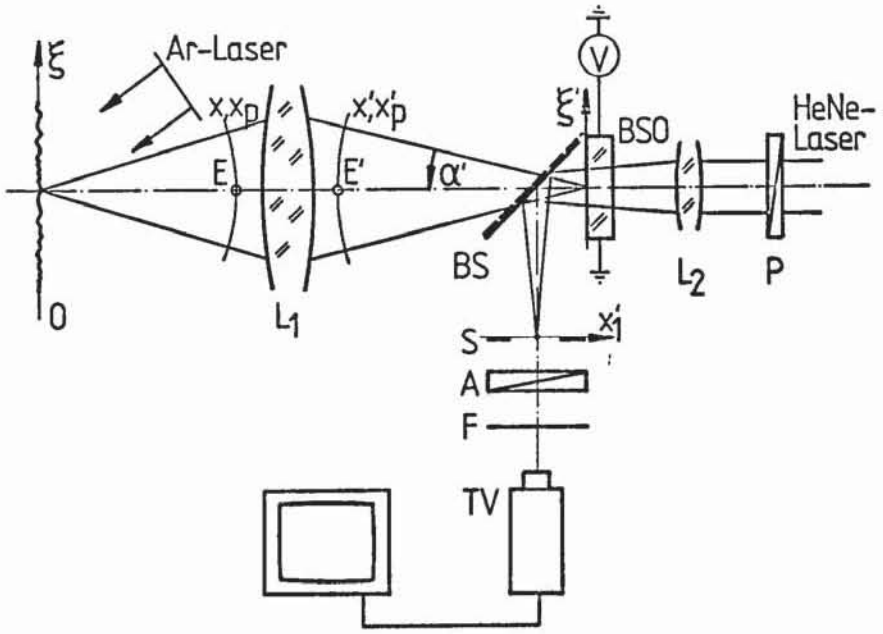

Fig. 6. Experimental arrangement for recording speckle pattern in the image-plane and displaying Young's fringes in real time.

We can therefore write the amplitude immediately in front of the crystal illuminated with a plane wave A'_o of wavelength

$$A'(\vec{\xi}', \Delta\vec{\xi}') \approx C\, A'_o \{1 + i \frac{2\pi}{\lambda_1} \Delta\vec{n}\cdot\vec{d}\} \quad .$$

We are now interested in the intensity in the Fourier-transform plane $|a_1(\vec{x}_1)|^2$

$$|a_1(\vec{x}_1)|^2 = C_1 \left\{\delta(\vec{x}'_1) + \left|\frac{2\pi}{\lambda_1} d\cdot\Delta n_s \frac{\psi \circledast \psi^*}{\langle I(\xi')\rangle}\right|^2 \left(1+\cos\frac{2\pi \vec{x}'_1\cdot\Delta\vec{\xi}'}{\lambda_2 f'_2}\right)\right\} \qquad (4)$$

The object displacement $\Delta\vec{\xi}$ is given by the fringe spacing in the Fourier-transform plane

$$|\Delta(\xi)| = \frac{f'_2 \lambda_2}{M |x'_c|} \quad . \qquad (5)$$

C and C_1 are constants taking into account the absorption, and the reflection loss at the crystal interfaces for λ_1 and λ_2, $\psi \circledast \psi^*$ is the autocorrelation of the pupil of the image forming lens L_1 in fig. 6.

x'_c = fringe spacing

f'_2 = focal length of the lens forming the Fourier-transform or the separation between crystal and Fraunhofer-plan when the crystal is illuminated with a spherical wave.

A similar analysis applies for tilt analysis where the speckle pairs are no longer recorded in the image plane but in the Fourier-transform plane of the lens L_1 in fig. 6. Speckle photography for tilt analysis is described by Gregory[5] and Tiziani[6]. From the fringe spacing the angular tilt γ can be found

$$\gamma = \frac{f'_2}{f'_1} \frac{\lambda_2}{(1+\cos\beta)|x'_c|} \quad . \qquad (6)$$

f'_1 = focal lens of the lens L_1
f'_2 = focal lens of the lens L_2 as in equation (5)
β = angle of incidence of the plane wave illuminating the object.

Furthermore, the speckle pattern of an oscillating object can also be recorded in the time average i.e. the BSO is illuminated during a number of oscillating cycles.

4. Experimental results with BSO crystal used for speckle pattern recording

A typical arrangement for deformation-, displacement and vibration analysis in real time is shown in fig. 6. The optically rough surface is illuminated with an Argon laser (λ_1 = 514 nm). The lens L_1 forms the image of the object into the crystal for in-plane analysis. The power needed to write the speckle pattern in the crystal was 20 $\mu W\ cm^{-2}$ and the cycling time $\leq$1 sec. For speckle application, the crystal thickness was chosen to be smaller than for holography to reduce the Bragg volume effect. For reading out the information and displaying the Young's fringes in the Fraunhofer-plane, a 1 mW HeNe-laser was used. In the Fraunhofer-plane a stop is inserted to eliminate the undiffracted light. Furthermore, an analyzer and polarizer was found to be very useful to eliminate unwanted light. The Young's fringes are formed on a TV-screen. The fringes can be analysed directly using TV techniques as indicated in fig. 8. Fig. 7 shows the results obtained from a double exposed speckle pattern with a displacement of 80 µm between the two exposures.

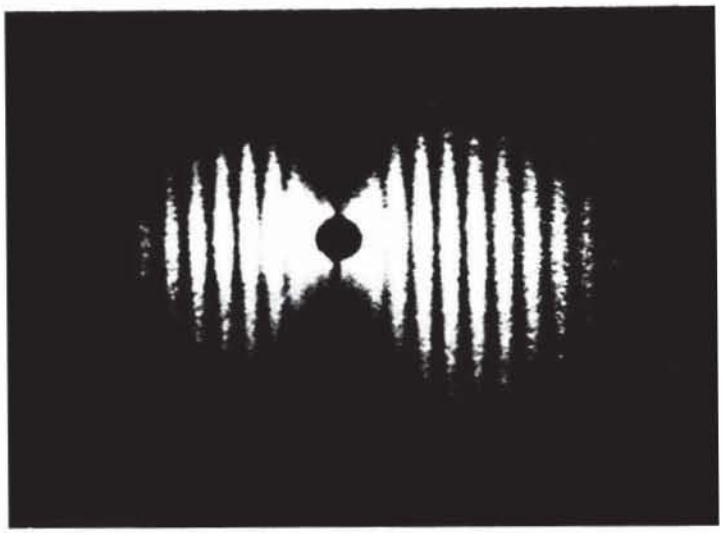

Fig. 7. Young's fringes obtained by recording the double exposure speckle pattern in the image plane with a displacement of 80 µm.

Fig. 8 shows tilt fringes of an work piece illuminated in reflection with a plane wave.

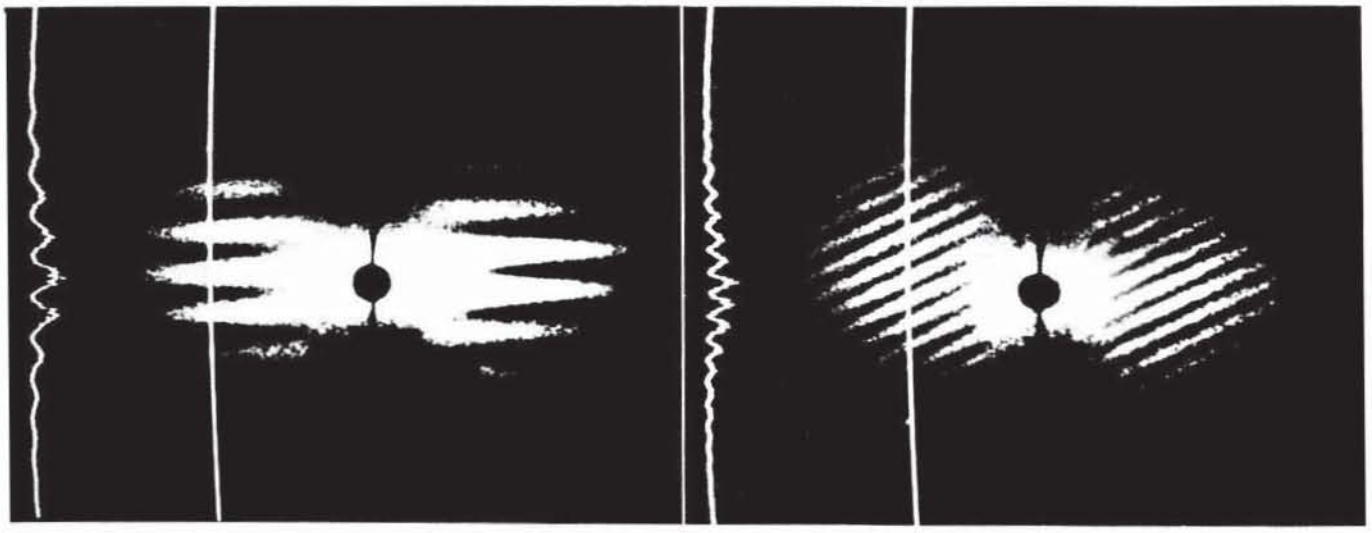

Fig. 8. Young's fringes obtained by the double exposure speckle pattern in the Fourier-transform plane with tilts of
a) 25 sec of arc between the two exposures and a horizontal axis of tilt
b) 50 sec of arc between the exposures and tilt axis at 23 degree to the horizontal axis.

The double exposure speckle pattern was recorded in the Fourier transform-plane of lens L_1 in fig. 6. Tilts of 25 sec of arc and 50 were introduced between the exposures in different azimuths. In fig. 9 results of an oscillating object recorded in the time average are displayed.

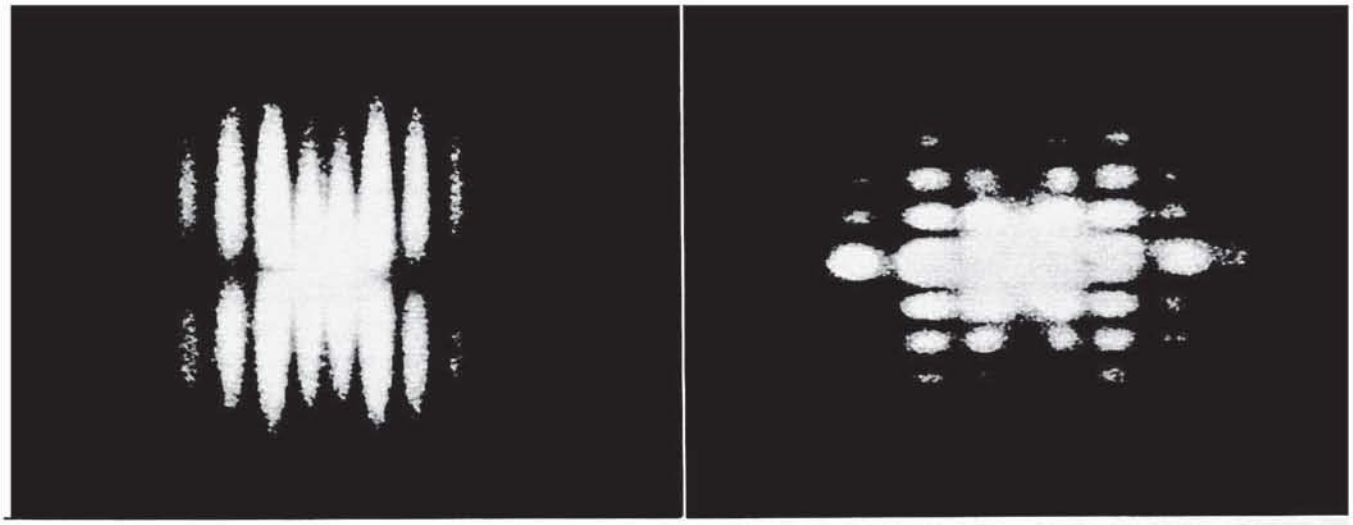

Fig. 9. Fringes obtained by recording time averaged speckle patterns in a BSO crystal
a) amplitude of oscillation ρ = 15 µm in horizontal direction
b) amplitude of oscillation ρ = 15 µm in vertical direction with an additional lateral displacement in the horizontal direction of 15 µm.

The speckle pattern stored during roughly 1 sec of the object oscillating at 1 kHz was recorded in a BSO crystal of 1 mm thickness. In the Fraunhofer-plane fringes can be observed following no longer the sinusoidal but intensity repartition of J_o^2, the Besselfunction J_o of order zero; in fig. 9a the amplitude of oscillation was 15 µm in a horizontal direction and in fig. 9b it was again 15 µm but in a vertical direction and a displacement of 15 µm was introduced horizontally. In fig. 9b the two fringe systems in the vertical and horizontal direction are different. In fig. 9a the zero order fringe is divided in two subfringes because of the halo as seen in fig. 7.

Conclusions

"Speckle photography" can now be applied in quasi real time for displacement, tilt and vibration analysis. The BSO storage material proved to be very promising with unlimited recycling. By displaying the speckle patterns with a wavelength different to the recording one, no storage device is required and TV techniques can be used directly for the fringe analysis.

We would like to thank the DFG for the financial support of the work.

References

1. Huignard, J. P., Micheron, F., "High sensitivity read-write volume holographic storage in Bi_{12} Si O_{20} and Bi_{12} Ge O_{20} crystals", Appl. Phys. Lett., Vol. 29, pp. 591-593. 1976.
2. Huignard, J. P., Herriau, J. P., "Real-time double exposure interferometry with Bi_{12} Si O_{20} crystals in transverse electro-optic configuration", Appl. Optics, Vol. 16, pp. 1807-1809. 1977.
3. Tiziani, H. J., "Vibration analysis and deformation measurement in "Speckle metrology", pp. 73-109, Academic Press. 1978.
4. Tiziani, H. J., Leonhardt, K., Klenk, J., "Real-time displacement and tilt analysis by a speckle technique using Bi_{12} Si O_{20} crystals", Opt. Comm. in print.
5. Gregory, D. A., "Basic physical principles of defocused speckle photography: a tilt topology inspection technique", Opt. Laser Technol., Vol. 8, pp. 201-213. 1976.
6. Tiziani, H. J., "A study of the use of laser speckle to measure small tilts of optically rough surfaces accurately", Opt. Comm., Vol. 5, pp. 271-276. 1972.